11.6 ATMOSPHERIC WIND RETRIEVALS FROM SATELLITE SOUNDINGS OVER THE POLAR PLATEAU REGIONS

Cheng-Zhi Zou[1,2], Michael L. Van Woert[1,3], and Chuanyu Xu[3,4]

[1]*NOAA/NESDIS/Office of Research and Applications, Camp Springs, Maryland*

[2]*Joint Center for Satellite Data Assimilation, Camp Springs, Maryland*

[3]*U.S. National Ice Center, Washington , D.C.*

[4]*QSS Group, Inc., Lanham, Maryland*

1. Introduction

In an attempt to derive the atmospheric wind profiles from satellite observations, Zou and Van Woert (2002) have demonstrated that the satellite-derived atmospheric general circulation resulting from the TOVS Pathfinder A temperature profile (Susskind et al. 1997) plus a SSM/I-based surface wind field (Atlas et al. 1996) exhibits structure similar to the NCEP-NCAR and ECMWF reanalysis winds over the Southern Ocean. In addition, the satellite-derived wind profiles compare favorably with the radiosonde observations at Macquarie Island with an annual mean bias of near 1 m sec^{-1} for both the zonal and meridional wind components. These results suggest a potentially significant benefit in using the satellite-derived winds as an alternative independent source to the NCEP-NCAR and ECMWF reanalysis winds for climate studies over the Polar Regions. This is particularly true given that the NCEP-NCAR and ECMWF reanalysis winds exhibit large errors when validated against independent radiosonde observations (Francis, 2002) and diverse climate variability (e.g., Bromwich et al. 2000) when used for moisture transport studies over the Polar Regions.

In Zou and Van Woert (2002, referred to as ZVW02 hereafter), however, the satellite wind retrieval schemes were designed only for the open flat ocean conditions. In this study, a general surface boundary condition is included in their scheme so that their method can be used to retrieve the atmospheric winds over plateaus such as the Antarctic continent and Greenland. The resultant atmospheric general circulation structure is then compared with the NCEP-NCAR Reanalysis-2 (Kistler et al. 2001) winds over the Antarctic coastal region.

Corresponding author address: Dr. Cheng-Zhi Zou, Office of Research and Applications, NOAA/NESDIS, NOAA Science Center, Room 711, 5200 Auth Road, Camp Springs, MD 20746
E-mail: cheng-zhi.zou@noaa.gov

2. Data

The satellite data used in this study are the same as in ZVW02. The surface wind field is the blended SSM/I-ECMWF analysis wind obtained by Atlas et al. (1996). This surface wind is available globally every 6 hour since July 1987 with a spatial resolution of 2^0 latitude by 2.5^0 longitude. Since the SSM/I surface wind speed is available only over the oceans, the blended surface wind over land is dominated by the ECMWF analysis. The temperature data were taken from the TOVS Pathfinder Path A dataset (Susskind et al. 1997). Daily mean virtual temperature retrievals from the TOVS Path A are available globally on a 1^0x1^0 latitude and longitude grid. These temperature data are defined at the layers of 1000 to 850, 850 to 700, 700 to 500, 500 to 300, and 300 to 100 hPa. All data are interpolated onto a 2^0 latitude by 2.5^0 longitude grid with a 6-hour interval.

3. Derivation of satellite wind

Over the middle and high latitudes, the thermal wind equations are good approximations to the momentum equations. The thermal wind equations and the continuity equation for an atmosphere in hydrostatic balance in spherical and isobaric coordinates are written as

$$\frac{\partial u_g}{\partial \ln p} = \frac{R_d}{f}\frac{\partial T^v}{a\partial\varphi} \tag{1}$$

$$\frac{\partial v_g}{\partial \ln p} = -\frac{R_d}{f}\frac{\partial T^v}{a\cos\varphi\partial\theta} \tag{2}$$

$$\nabla \bullet \mathbf{V} + \frac{\partial \omega}{\partial p} = 0 \tag{3}$$

where a is the Earth's radius, f the Coriolis parameter, R_d the dry air gas constant, T^v the virtual temperature, θ the longitude, φ the latitude, p the pressure; $\mathbf{V}$ is the

horizontal wind vector with the zonal and meridional components u and v; ω is the vertical p velocity; and u_g and v_g are the geostrophic zonal and meridional wind speeds, respectively. The top and bottom of the model atmosphere are assumed to be $p=p_T$ = 100 hPa and p = p_s, respectively. The surface wind is assigned to the p_s level. This study differs from ZVW02 in that p_s was fixed to be 1000 hPa in ZVW02, but here p_s can be any value. For instance, over the plateau areas such as the Antarctic continent or Greenland, the surface pressure can be as low as 650 hPa (Fig. 1). The satellite retrieved surface pressure is currently unavailable; therefore, we use the 12-hour surface pressure data from the ECMWF analysis. The boundary conditions for no

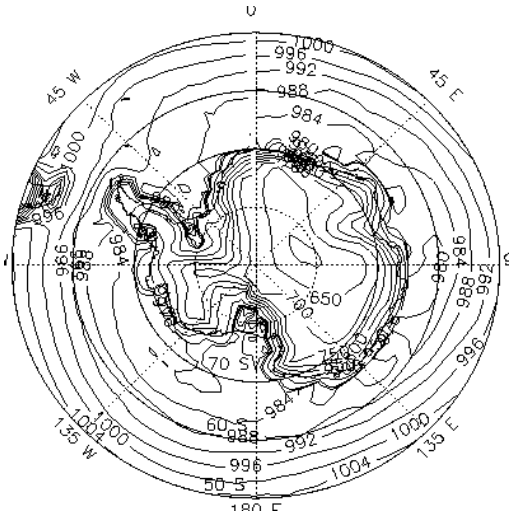

Fig. 1 1988 ECMWF analysis surface pressure near Antarctica.

mass transport through the boundaries are simply

$$\omega = 0 \quad \text{at} \quad p=p_T \tag{4}$$

and

$$\omega_s = \frac{dp_s}{dt} = \frac{\partial p_s}{\partial t} + \mathbf{V}_s \bullet \nabla p_s \text{, at } p = p_s \tag{5}$$

Since the surface wind and pressure data are given in this study, the vertical surface pressure velocity, ω_s , is also known through (5).

The vertical velocity in (3) can be eliminated through integration over p from the surface to the top of the model atmosphere. Using (Trenberth 1991)

$$\nabla \bullet \int_{p_T}^{p_s} \mathbf{V} dp = \int_{p_T}^{p_s} \nabla \bullet \mathbf{V} dp + \mathbf{V}_s \bullet \nabla p_s \tag{6}$$

the resultant mass conservation equation in a vertical atmospheric column is obtained as

$$\nabla \bullet \int_{p_T}^{p_s} \mathbf{V} dp = -\omega_s ' = -\frac{\partial p_s}{\partial t} \tag{7}$$

As in ZVW02, it is convenient to express (7) in a vertical differencing form. Using the trapezoidal rule and assuming N+1 vertical atmospheric levels, after manipulating the vertical indexes, (7) can be written as

$$\frac{\partial}{a\cos\varphi \partial\theta}\left(\sum_{k=k_s}^{N} f_k u_k\right) + \frac{\partial}{a\cos\varphi \partial\varphi}\left(\sum_{k=k_s}^{N} f_k v_k \cos\varphi\right) = -\omega_s ' \tag{8}$$

where the wind components have been introduced into the wind vector, and

$$f_k = \begin{cases} 0.5\Delta p_{k_s}, & k = k_s \\ 0.5(\Delta p_k + \Delta p_{k-1}), & k = k_s + 1,\ldots N-1 \\ 0.5\Delta p_{N-1}, & k = N \end{cases} \tag{9}$$

k is the vertical level index, k_s the index for the surface level (which is a function of both latitude and longitude), $\Delta p_k = p_k - p_{k+1}$ is the pressure difference between the two adjacent levels k and $k+1$, and $p_{ks}=p_s$. The design of the vertical differencing grid is illustrated in Fig. 2.

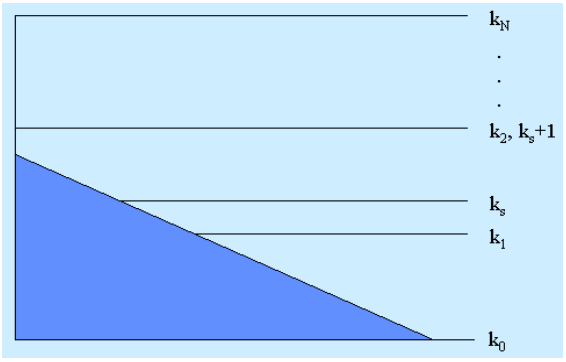

Fig. 2 Schematic showing the vertical differencing grid. The surface index k_s can be anywhere between the integral indexes k_0, …k_N. The integral index immediately above k_s is denoted as k_s+1, and other integral indexes above the surface are k_s+2,… k_N.

Integrating (1) and (2) with respect to p from the surface p_s to any level p_k, the resultant integral equations are

$$\tilde{u}_k = u_s + \int_{p_s}^{p_k} \frac{R_d}{f} \frac{\partial T^v}{a\partial\varphi} d\ln p, \quad k = k_s + 1,\ldots N \tag{10}$$

$$\tilde{v}_k = v_s - \int_{p_s}^{p_k} \frac{R_d}{f} \frac{\partial T^v}{a\cos\varphi \partial\theta} d\ln p, \quad k = k_s + 1, \ldots N \tag{11}$$

where u_s and v_s are the observed surface winds, $\tilde{u}$ and $\tilde{v}$ are the first-guess wind profiles Slonaker and Van Woert (1999). These winds are nonmass-conserved (ZVW02) and exhibit large biases when compared to the radiosonde observations. Therefore, a variational formalism is needed to force these winds to conserve mass. ZVW02 has presented two methods to construct the variational functional: deriving the zonal and meridional winds separately or simultaneously. They had demonstrated that the 'separate' method reduced the biases inherent in both the zonal and meridional components of the first-guess field, while the 'simultaneous' method does not reduce the bias in the first-guess zonal wind. Therefore, only the 'separate' method is used in this study.

Integrating (8) over a zonal circle and over latitude from a pole to a latitude φ, given that $\cos\varphi$ is zero at the poles, one obtains the following equation for the total net mass transport through a latitudinal wall,

$$\int_0^{2\pi} \sum_{k=k_s}^{N} f_k v_k a\cos\varphi d\theta = -\int_0^{2\pi} \int_{-\pi/2}^{\varphi} \omega_s'(\theta,\eta)\, a\cos\eta\, d\theta\, d\eta = -\overline{\omega}_s'(\varphi) \tag{12}$$

where η is an integration variable. Following ZVW02, the variational formalism for obtaining the mass-conserved meridional wind, v, is to minimize the differences between v and $\tilde{v}$ in a least-squares sense subject to the mass transport constraint Eq. (12), i.e.,

$$E = \int_0^{2\pi} \sum_{k=k_s+1}^{N} \alpha_k (v_k - \tilde{v}_k)^2 a\cos\varphi d\theta + \lambda_v \left[\int_0^{2\pi} \sum_{k=k_s}^{N} f_k v_k\, a\cos\varphi d\theta + \overline{\omega}_s'(\varphi)\right] \tag{13}$$

where λ_v is a Lagrange multiplier and α_k is a priori specified weighting function. To be consistent with the differencing scheme in the second term of the right-hand-side in Eq. (13), Wu et al. (2003) suggest that the weighting function should be expressed as

$$\alpha_k = \frac{f_k}{2\beta_k} \tag{14}$$

where β_k is the expected error covariance of $\tilde{v}$. ZVW02 assume the weighting function to be one throughout the atmosphere, i.e., α_k=1, which is equivalent to β_k=0.5 f_k. This resulted in a wind structure comparable to the radiosonde observations at Macquarie Island. Wu et al. (2003) further suggest that α_k=0.5 at the 100 hPa level and α_k=1 everywhere else, which resulted in a better representation of atmospheric circulation structure over the Southern Ocean, especially near the tropopause. This is because the error covariance of $\tilde{v}$ at 100 hPa is expected to be larger than other levels. To provide a direct comparison with ZVW02, and because there is considerable uncertainty in the vertical structure of β_k, in this study, β_k is chosen to be equal to 0.5 f_k, or α_k=1. The exact vertical structure of β_k over the Polar Regions can be determined by comparing the wind retrievals with the radiosonde observations over the same regions and is a topic of future study.

When (14) is used, the Euler-Lagrange equations for (13) give the following solution for v_k,

$$v_k = \tilde{v}_k - \beta_k \lambda_v, \qquad k=k_s+1, k_s+2, \ldots, N. \tag{15}$$

where λ_v is obtained by introducing (15) into (12), giving

$$\lambda_v = \frac{\int_0^{2\pi} \sum_{k=k_s}^{N} f_k \tilde{v}_k a\cos\varphi\, d\theta + \overline{\omega}_s'(\varphi)}{\int_0^{2\pi} \overline{\beta}(\theta) a\cos\varphi d\theta} \tag{16}$$

where $\overline{\beta}(\theta) = \sum_{k=k_s+1}^{N} \beta_k f_k$. Eqs. (11), (15) and (16) provide a complete solution for the mass-conserved meridional wind. When β_k is chosen to be 0.5 f_k, these solutions differ from ZVW02 only in that the surface index k=0 in ZVW02 is replaced by k_s and an additional term $\overline{\omega}_s'(\varphi)$ appears in the solution equation (16) for λ_v. Normalizing Eq. (12) by dividing by the surface pressure and the length of the zonal circle suggests that $\overline{\omega}_s'(\varphi)$ on the order of 1 mm sec^{-1}, since it balances the zonally and vertically averaged, mass-conserved meridional velocity (ZVW02). This is at least two orders of magnitude smaller than the zonally and vertically averaged speed of the nonmass-conserved wind $\tilde{v}$ (Zou and Van Woert 2001), therefore, it can be ignored in (16).

Assuming the meridional wind is now known, the zonal wind, u, can be obtained similarly by a variational formalism in which the differences between u and $\tilde{u}$ are minimized in a least-squares sense subject to the mass conservation constraint (8). The variational formalism at any latitude, φ, using Eq. (8) as a strong constraint is written as

$$E = \int_0^{2\pi} \alpha_k \sum_{k=k_s+1}^{N} (u_k - \tilde{u}_k)^2 a\cos\varphi d\theta +$$
$$\int_0^{2\pi} \lambda_u [\frac{\partial}{a\cos\varphi \partial\theta} (\sum_{k=k_s}^{N} f_k u_k) +$$
$$\frac{\partial}{a\cos\varphi \partial\varphi} (\sum_{k=k_s}^{N} f_k v_k \cos\varphi) + \omega_s'] a\cos\varphi d\theta \quad (17)$$

Taking the first variation of (17), integrating by parts, and using the periodic boundary conditions $\lambda_u(0)=\lambda_u(2\pi)$ as in ZVW02, the Euler-Lagrange equation of (17) leads to a pair of equations. One of them is the constraint equation (8), and the other is the following solution for u_k,

$$u_k = \tilde{u}_k + \beta_k \frac{\partial \lambda_u}{a\cos\varphi \partial\theta}, k = k_s + 1, k_s + 2, ...N \quad (18)$$

where Eq. (14) has been used. Introducing (18) into (8), after manipulating the equation, it is reduced to a second order ordinary differential equation for λ_u,

$$\frac{\partial}{\partial\theta} (\bar{\beta} \frac{\partial \lambda_u}{\partial\theta}) = -a\cos\varphi \{ \frac{\partial}{\partial\theta} (\sum_{k=k_s}^{N} f_k \tilde{u}_k) + \frac{\partial}{\partial\varphi} (\sum_{k=k_s}^{N} f_k v_k \cos\varphi) + a\cos\varphi \omega_s' \} \quad (19)$$

Because $\tilde{u}$, v and ω_s' are already known, the right hand side of (19), denoted as $H(\theta,\varphi)$, is known. Direct integration of (19) gives the solution for λ_u,

$$\lambda_u = \int_0^{\theta} \bar{\beta}^{-1} G(\gamma,\varphi) d\gamma + C_0 \int_0^{\theta} \bar{\beta}^{-1} d\gamma + C_1 \quad (20)$$

where C_0 and C_1 are as yet undetermined constants, γ is an integration variable, $G(\theta,\varphi) \equiv \int_0^{\theta} H(\gamma,\varphi) d\gamma$. Utilizing the periodic boundary condition $\lambda_u(0)=\lambda_u(2\pi)$, C_0 can be determined as

$$C_0 = -\frac{\int_0^{2\pi} \bar{\beta}^{-1} G(\gamma,\varphi) d\gamma}{\int_0^{2\pi} \bar{\beta}^{-1} d\gamma} = -\bar{G}(\varphi) \quad (21)$$

where $\bar{G}(\varphi)$ is the zonally averaged $G(\theta,\varphi)$ with a weighting function of $\bar{\beta}^{-1}$.

Using (21), the first-order derivative of (20) becomes

$$\frac{\partial \lambda_u}{\partial\theta} = \bar{\beta}^{-1} [G(\theta,\varphi) - \bar{G}(\varphi)] \quad (22)$$

Because only $\partial\lambda_u/\partial\theta$ is needed in the zonal wind solution (18), the unknown constant C_1 does not need to be determined.

The above procedure gives a complete solution for the mass-conserved meridional and zonal winds provided the temperature soundings and surface wind fields are known. Similar to the case for λ_v, dimensional analysis shows that the ω_s' term in Eq. (19) can be ignored as well.

4. Results

Figures 3 and 4 show comparisons between the satellite-derived annual mean winds for 1988 and the corresponding NCEP-NCAR Reanalysis-2 winds near the Antarctic coast at the surface, 700 mb, and 500 mb. At the surface, both the blended SSM/I-ECMWF and the NCEP-NCAR Reanalysis-2 winds show similar kabatic wind patterns in which the cold heavy air inside the continent interior blows outward over the warmer oceans (e.g., Parish and Bromwich, 1991). At 700 mb, the wind structure over the eastern Antarctic continent (approximately 70^0S to 76^0S) is similar to the surface for both the satellite-derived and the NCEP-NCAR Reanalysis-2, a reflection that the surface pressure is close to 700 mb in that region (Fig.1). However, near the western coast of Weddell Sea and the western coast of Ross Sea, significant differences occur between the satellite-derived and the NCEP-NCAR Reanalysis-2 winds. In particular, the satellite winds tend to blow in a direction such that the Antarctic continent is on its right side. For instance, near the western coast of Weddell Sea, the wind vector is toward the southern-east, and over the western coast of Ross Sea the wind direction is toward the South Pole. These wind directions appear to be opposite to the NCEP-NCAR Reanalysis-2 winds over the same regions. At 500 mb, large differences between the satellite-derived and NCEP-NCAR Reanalysis-2 winds occur over the entire Antarctic coastal regions. These differences over the Weddell Sea and the Ross Sea are similar to those observed at 700 mb. Near the eastern Antarctic coast, however, the satellite-derived winds show a profound vortex structure following the curvature of the Antarctic coastline (e.g., 45^0E-90^0E near 70^0S). Again, the winds blow in such a direction that the Antarctic continent is on its right side. Overall, these 500 mb satellite-derived wind patterns correspond very well with the contour patterns of the TOVS surface-500 mb mean temperature (Fig. 3c). These correspondences suggest a mid-troposphere thermal wind structure for the Antarctic coastal winds. In particular, the temperature over the Antarctic continent is much lower than that over the ocean, causing a strong temperature gradient across the coastline. This temperature gradient results in a strong thermal wind vector with colder air lying to its right in

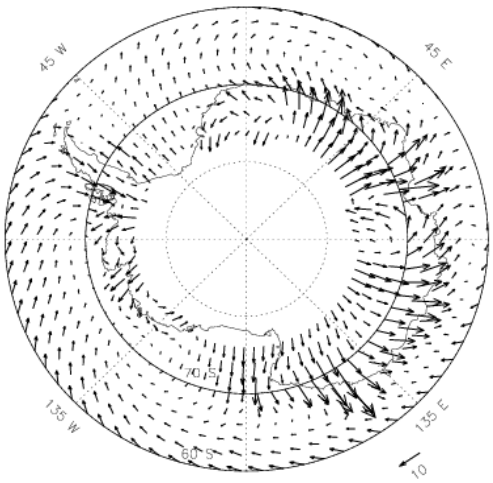

(a)

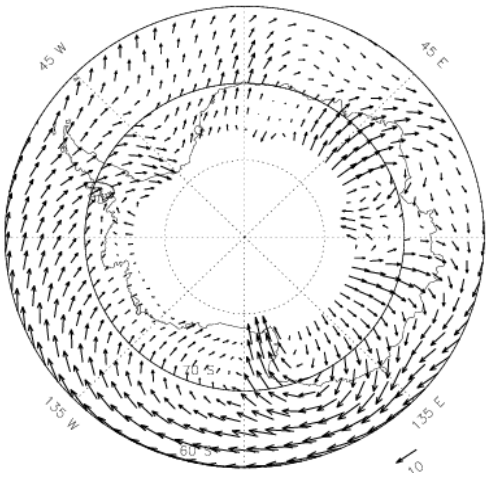

(b)

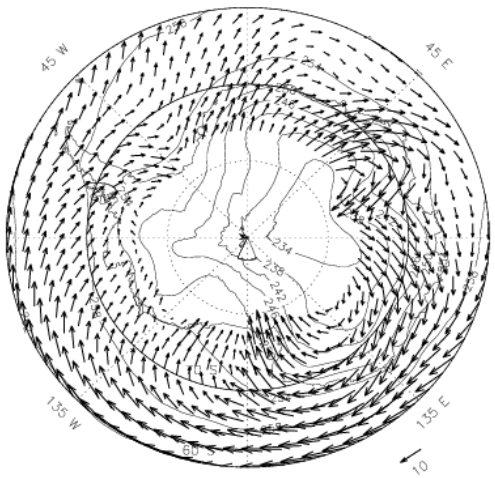

(c)

Fig. 3 Satellite-derived annual mean wind near Antarctica for 1988. (a) Surface; (b) 700 mb; (c) 500 mb wind and the 1988 surface-500mb mean temperature from TOVS Pathfinder A.

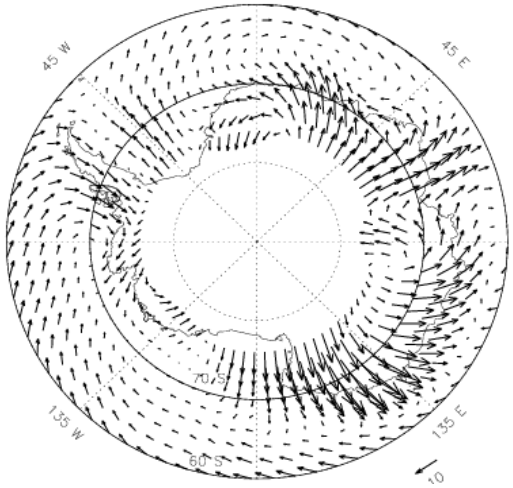

(a)

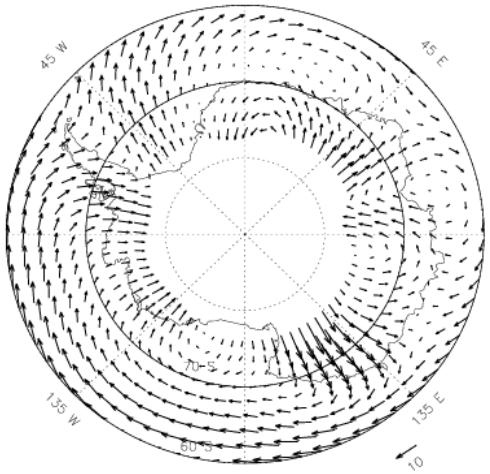

(b)

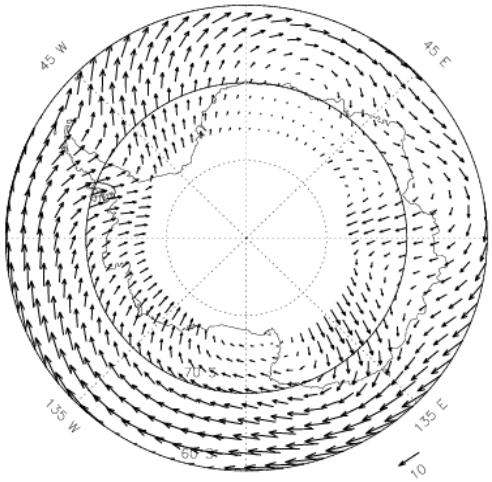

(c)

Fig. 4 1988 annual mean NCEP-NCAR Reanalysis-2 wind field near Antarctica. (a) Surface; (b) 700 mb; (c) 500 mb.

the Southern Hemisphere. Since the thermal wind is the wind difference between the upper and lower levels, the upper level wind is the summation of the thermal wind and the lower level wind. Therefore, Fig. 3c suggests that the thermal winds are so strong that, after they were added to the surface wind, the winds at the upper level still exhibit similar directions to the thermal winds.

In contrast to the satellite winds, however, the Reanalysis-2 500 mb winds fail to show many of the fine structure of the thermal winds. Further analyses will be carried out to understand the reasons for these differences.

REFERENCES

Atlas, R., R. N. Hoffman, S. C. Bloom, J. C. Jusem, and J. Ardizzone, 1996: A multi-yearglobal surface wind velocity dataset using SSM/I wind observations*, Bull. Amer. Meteorol. Soc*., **77**, 869-882.

Bromwich, D., A. N. Rogers, P. Kållberg, R. I. Cullather, J. W. C. White, and K. J. Kreutz, 2000: ECMWF analyses and reanalyses depiction of ENSO signal in Antarctic Precipitation. *J. Climate*, **13**, 1406-1420.

Francis, J. A.,2002: Validation of reanalysis upper-level winds in the Arctic with independent rawinsonde data, *Geophys. Res. Let*., **29**, 1-4.

Kistler, R., and Coauthors, 2001: The NCEP-NCAR 50-year reanalysis: monthly means CD-ROM and documentation, *Bull. Amer. Meteorol. Soc.*, **82**, 247-267.

Parish, T. R., and D. H. Bromwich, 1991: Continental-scale simulation of the Antarctic katabatic wind regime. *J. Climate*, **4**,135-146.

Slonaker, R. L., and M. L. Van Woert, 1999: Atmospheric moisture transport across the Southern Ocean via satellite observations, *J. Geophys. Res*., **104**, 9229-9249.

Susskind, J, P. Piraino, L. Rokke, L. Iredell, and A. Mehta, 1997: Characteristics of the TOVS Path A dataset, *Bull. Amer. Metorol. Soc*., **78**. 1449-1472.

Trenberth, K. E., 1991: Climate diagnostics from global analysis: Conservation of mass in ECMWF analysis, *J. Climate*, 4, 707-722.

Wu, X., C.-Z. Zou, M. Van Woert, and C. Xu, 2003: The influence of the error covariance structure on the satellite-derived atmospheric circulation over the Southern Ocean, *Seventh Conf. On Polar Meteorology and Oceanography*, Hyannis, MA, Amer. Meteor. Soc.

Zou, C.-Z., and M. Van Woert, 2001: The role of conservation of mass in the satellite-derived poleward moisture transport over the Southern Oceans. *J. Climate,* **14**, 997-1016.

Zou, C.-Z., and M. Van Woert, 2002: Atmospheric wind retrievals from satellite soundings over the middle and high latitude oceans, *Mon. Wea. Rev*., **130**, 1771-1791.